Experiments in Fiber Optics

Maitrey Sharma*
School of Physical Sciences,
National Institute of Science Education and Research,
HBNI, Jatni-752050, India.

(Dated: November 28, 2022)

In this experiment, we have undertake various experiments concerning optical fibers, the backbone of modern communications systems. We begin by understanding the handling of the fibers using tools and how to prepare them for experiments. We classify between different kinds of optical fibers (single-mode and multi-mode) and carefully explore how they are affected differently in various experiments. We calculate numerical apertures, mode-field diameters, and micro- and macro-bending losses in the fibers to build a greater understanding of their working.

I. INTRODUCTION

In the early 1840s Paris, Daniel Colladon and Jacques Babinet first demonstrated the guiding of light by refraction and by the 19th century, a team of doctors from Vienna were able to guide light through bent glass rods to illuminate body cavities. Over the next century practical applications followed and in 1953, Dutch scientist Bram van Heel first demonstrated image transmission through bundles of optical fibers with a transparent cladding.

Today, optical fibers form the backbone of our communications systems, permitting transmission of data over longer distances and at higher bandwidths (data transfer rates) than electrical cables. They suffer less loss and suffer less electromagnetic interference than their metal counterparts. Their usage extends beyond data transmission to various specialized instrumentations like sensors and lasers.

Optical fibers typically include a core surrounded by a transparent cladding material with a lower index of refraction. Light is kept in the core by the phenomenon of total internal reflection which causes the fiber to act as a waveguide. Fibers that support many propagation paths or transverse modes are called *multi-mode fibers*, while those that support a single mode are called *single-mode fibers*.

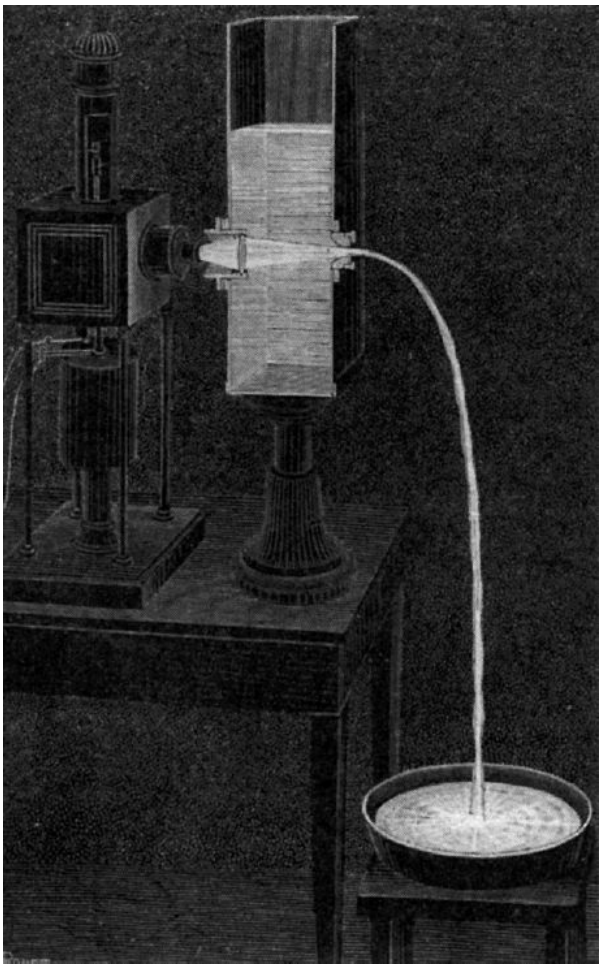

FIG. 1: An illustration of Colladon's *light fountain* from one of his publications.

II. OBJECTIVES

There are several major objectives that will be achieved as part of this experiment. They are:

1. The preparation of an optical fiber for experiments will be understood.
2. We will calculate numerical aperture of both single-mode and multi-mode fibers.
3. We will calculate the mode field diameter of a single-mode fiber.
4. We will be studying the effects of microbending loss and will explore its applications in sensing for multi-mode fibers.
5. Finally, we will also be studying the mechanics of

* maitrey.sharma@niser.ac.in;
Roll No.: 1911093

FIG. 2: He-Ne laser with aligners in place

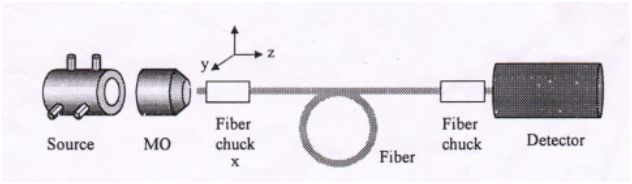

FIG. 3: Experimental setup for launching light from a laser diode into an optical fiber using an MO.

bend-induced in a single-mode fiber.

III. EXPERIMENTAL SETUP

The setup uses an optical breadboard to mount all the necessary equipment, which includes a helium-neon laser source, aligners for the source (see Figure 2), a microscopic objective (40X), microscopic objective holder, transnational stages with chucks (fiber positioners) mounted on them, a photo-detector connected to a multimeter, a photo-detector holder, and posts and holders as needed. In addition to this, along the single-mode and multi-mode fibers, we used a fiber stripper to remove the cladding of the fibers, a fiber cutter and an index matching liquid to clean the fiber ends before coupling them with the laser.

The final setup, in its idealized state, looks like as shown in Figure 3.

Our initial setup was not optimal. The mounts were wobbly and it was difficult to stabilize them and maneuvering them precise alignment which is needed for coupling the fiber with the laser. In the setup that we inherited from the previous group who worked there was

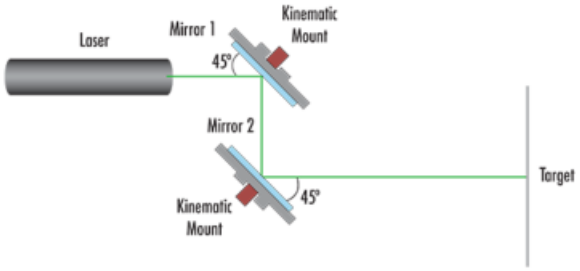

FIG. 4: The Z-fold configuration in laser alignment techniques

only one holder (or aligner) to adjust the laser source, but we discovered that it was not stable enough. To solve this, we fitted one more aligner but that made the whole source to rigid, leaving us out of any way to align it.

Our Innovation to improve the setup

The process of alignment consists of four components that need to be aligned with each other: the source itself, the microscopic objective (MO), the fiber, and then the detector. Here, the alignment of source with the MO and that of fiber with the detector is trivial. However, aligning the MO with the fiber requires precision. To reacquire fine control to align the our setup, we mounted two mirrors in the Z-fold configuration (see Figure 4). Now we could use the kinetic mounts of the mirrors we used (see Figure 5) for precise alignment. We also used apertures (irises) to align the laser further down the optical breadboard. Through this z-fold configuration we created a very robust setup which was then easily aligned.

There were some more problems with the setup, such as faulty translation stages, due to which we had to skip few experiments, whereas nonavailability of a different type of laser source meant we could not do some specific experiments (more in Section V).

IV. THE EXPERIMENTS

A. Fiber-end preparation and coupling

Before taking any measurements, we need to ensure that the end-faces of the fibre are perpendicular to the axis of the fibre. We strip the cladding on both the fibre ends, over a very short distance. Then we clean it with isopropyl alcohol. Then for end preparation a high precision cleaver was used. If required, a very small amount of oil (or any high refractive index fluid) might be put on the ends to remove cladding modes.

For coupling, we launch light from the laser diode onto the microscope objective (MO). The MO acts a lens,

FIG. 5: Mirrors used in the z-fold configuration with kinetic mounts

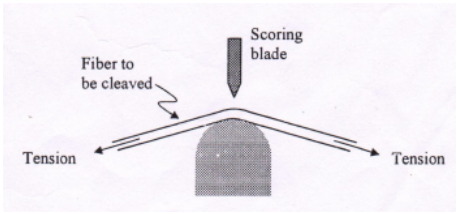

FIG. 6: Controlled-fracture of an optical fiber for its end-preparation through bend, score and break techniaue.

wherein the parallel rays of light from the laser are focused on a spot and transmitted to the optical fibre. To couple light from the source to the fibre, we need to ensure that the laser, MO and the fibre lie at the same vertical level. For this we measure the height of laser output using a scale at different distances and ensure it is the same. We also measure the height of the MO and fibre and keep it at the same level. We adjust the fine knobs on the translational stage until we get the maximum output.

B. Numerical Aperture measurements

In simplest terms, numerical aperture is a measurement of the ability of an optical fiber to capture light. All fibers have acceptance angle (which forms the acceptance cone of the guided ray). The numerical aperture (NA) of a fiber is defined as the sine of the largest angle an incident ray can have for total internal reflectance in the core. Rays launched outside the angle specified by a fiber's NA will excite radiation modes of the fiber.

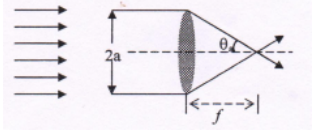

FIG. 7: lens representing a MO of focal length f and numerical aperture $\sin\theta_a$

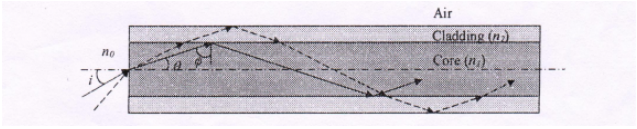

FIG. 8: Ray diagram illustrating the propagation of guided and cladding modes in an optical fiber

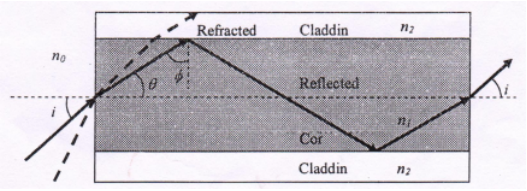

FIG. 9: A meridional ray entering a step index optical fiber at an angle $i < i_m$ gets guided through the fiber, and comes out at the same angle i from the output end of the fiber. Rays incident at angles $> i$, will get refracted into the cladding, eventually loosing all their energy in the cladding.

Therefore, we can define numerical aperture quantitatively as

$$NA = \sin i_m = \sqrt{n_1^2 - n_2^2} \tag{1}$$

where n_1 and n_2 are the refractive indices of the core and the cladding, respectively. Figure 9 shows the geometrcal ray path of a particular meridional ray in a step index multi-mode fiber.

The NA of the fiber is determined by measuring the angular dependance of the far field of the fiber. The far-field of the fiber represents the field distribution at any distance $z \gg (2a)^2/\lambda$ where a is the core radius of the fiber and λ is the operating wavelength. The semi-angle corresponding to 5% level of far field intensity maximum is the acceptance angle. The acceptance angle is given by:

$$i_m = \frac{\theta_2 - \theta_1}{2} \tag{2}$$

General Procedure

1. The detector is mounted on a rotational stage.
2. After end preparation and coupling, the maximum output is checked such that it lies at the 0° of the rotational stage.

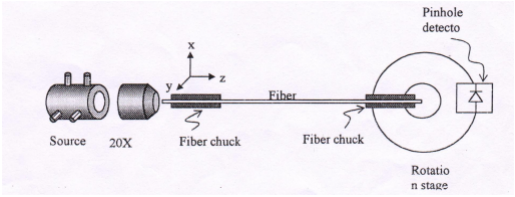

FIG. 10: Experimental setup for scanning the far-field intensity distribution of a fiber using a rotational translation stage.

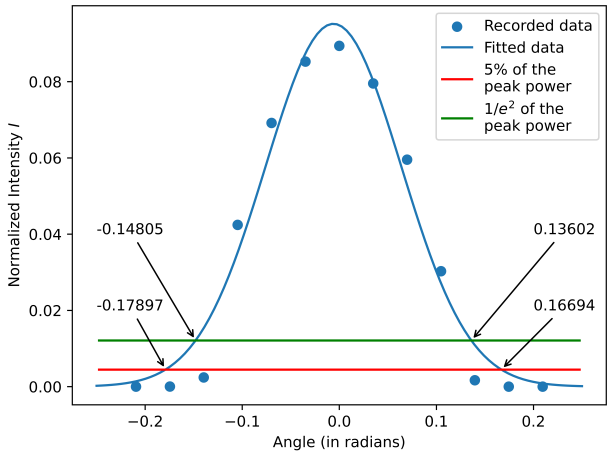

FIG. 11: Plot for single-mode numerical aperture and mode-field diamter calculation

3. The detector is rotated and the output is recorded.

4. The angle i_m at which intensity drops to 5% of the maximum value is measured and the acceptance angle is calculated.

1. *Single-mode fiber*

For single-mode fiber, we find that the intensity variation with detector being rotated through an angle followed the Gaussian curve. We found the intersection points with the 5% percent of the maximum intensity level at $\theta_1 = -0.17897$ and $\theta_2 = 0.16694$. Using equation 2, we got $\sin i_m = 0.172$ which is close to the actual value of 0.1 for the numerical aperture. This whole is plotted, fitted and labeled in Figure 11.

2. *Multi-mode fiber*

For multi-mode fiber, we realized that the source we had will not work because to measure the numerical aperture for the multi-mode fiber, we need to excite all the guided modes approximately equally by means of an incoherent Lambertian source[1], such as a tungsten halogen lamp (which unfortunately we could not obtain). It can be shown that the power accepted at any point r in the fiber core from a Lambertian source is directly proportional to square of the local numerical aperture.

Therefore, here we used the visual method to measure the numerical aperture and for the incoherent source, we employed a white light source. The reading are tabulated in Table II. We recorded $D = 2r$ versus z with the sources and used the following formulae

$$NA = \sin i_m = \sin[\tan^{-1}(D/2z)] \tag{3}$$

After recording the values, we calculated the average value of NA as 0.2310 which is close to the actual value of 0.2.

TABLE I: Recorded data for single-mode fiber numerical aperture measurement

Angle (in degrees)	Angle (in radians)	Voltage V (in volts)	Normalized Intensity ($\propto V^2$)
-12	-0.209	0	0.0000
-10	-0.175	0.004	0.0002
-8	-0.140	0.049	0.0269
-6	-0.105	0.206	0.4747
-4	-0.070	0.263	0.7737
-2	-0.035	0.292	0.9537
0	0.000	0.299	1.0000
2	0.035	0.282	0.8895
4	0.070	0.244	0.6659
6	0.105	0.174	0.3387
8	0.140	0.041	0.0188
10	0.175	0.003	0.0001
12	0.209	0	0.0000

TABLE II: Recorded data for multi-mode numerical aperture calculation

z (in)	z (cm)	r (cm)	NA	Average NA
2	5.08	1.3	0.2479	0.2310
3	7.62	1.8	0.2299	
5	12.7	3.1	0.2371	
6	15.24	3.6	0.2299	
7	17.78	4.1	0.2247	
8	20.32	4.5	0.2162	

[1] A Lambertian source is an optical source which obeys the Lambertian cosine law which states hat the radiant intensity or luminous intensity observed from an ideal diffusely reflecting surface or ideal diffuse radiator is directly proportional to the cosine of the angle θ between the direction of the incident light and the surface normal; $I = I_0 \cos(\theta)$.

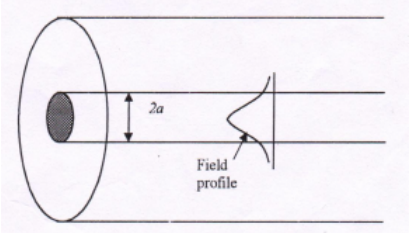

FIG. 12: Schematic diagram of the amplitude distribution of the propagating fundamental mode ina single-mode fiber

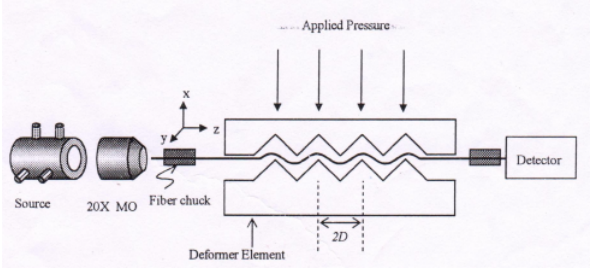

FIG. 13: Experimental set-up for a simple intensity modulated fiber optic pressure sensor using a multi-mode fiber

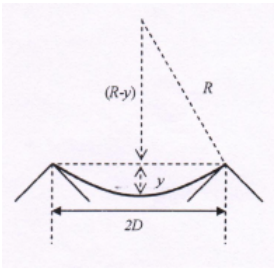

FIG. 14: Geometry of the microbend

C. Mode field diameter of a single-mode fiber

The mode field diameter (MFD) is a measure of the optical power per unit area, across the end face of a single-mode fiber. The most fundamental mode of the optical fibre is LP_{01} mode which can be approximated to have a Gaussian profile under the approximation of strong coupling. For any Gaussian beam, the spread is calculated by FWHM (full width half maximum) angle. The angle θ_e at which the far-field intensity drops down by a factor of e^2 from its maximum value at $\theta = 0$ would then be given by:

$$\tan\theta_e = \frac{\lambda}{\pi w_0} \tag{4}$$

which gives

$$w_0(\text{mode field radius}) = \frac{\lambda}{\pi \tan\theta_e} \tag{5}$$

General Procedure

Same steps as measurement of NA of Multimode fibre, with only one difference that at the ends of the single mode fibre we put a few drops of oil to prevent cladding modes.

Results

As annotated in the Figure 11, the $1/e^2$ value was found the angles $\theta_1 = -0.14805$ and $\theta_2 = 0.13602$. Therefore

$$\theta_e = \frac{0.14805 + 0.13602}{2} = 0.142035 \tag{6}$$

which gives $\tan\theta_e = 0.143$ and finally we get

$$w_0 = \frac{\lambda}{\pi \tan\theta_e} = \frac{632.8\,\text{nm}}{\pi \times 0.143} = 1.4\,\mu\text{m} \tag{7}$$

D. Microbending loss in a multi-mode fiber

In this experiment, we study intensity variation through a fiber by inducing microbends in the fiber through a periodic deformer element. When a portion of a fiber lay is sandwiched between two deformers and pressure is applied to one of these deformer, the fiber undergoes periodic deformation in the form of micro-bends. The resultant mechan- ical deformation of the optical fiber perpendicular to its axis causes higher-order guided modes to radiate out of the fiber's core through the core-cladding interface as shown in the figure. This results in a drop of intensity of the transmitted light through the fiber with increasing deformation. The loss is given as

$$\text{Loss} = C\left(\frac{a}{R}\right)^2 \tag{8}$$

From Figure 14,

$$R = \frac{y^2 + D^2}{2y} \tag{9}$$

where y is the displacement of the deformer element and $2D$ is the distance between the contact points of the deformer element, which is equal to the pitch of the element. Thus, the transmittance T through the fiber is

$$T = 1 - \text{Loss} = 1 - \frac{Ca^2}{\left(\frac{y^2 + D^2}{2y}\right)^2} \tag{10}$$

TABLE III: Recorded data for microbending loss in multi-mode fiber

Mass (in grams)	Voltage (in volts)	Normalized Intensity
0	0.325	1
106.17	0.291	0.8017
203.37	0.279	0.7370
299.73	0.276	0.7212
387.91	0.253	0.6060
486.68	0.247	0.5776
580.2	0.18	0.3067
675.58	0.046	0.0200

or

$$T = 1 - C'\left(\frac{q}{1+q^2}\right)^2 \tag{11}$$

where $C' = 4Ca^2/D^2$ and $q = y/D$. The applied force and hence the pressure is proportional to the displacementy. Therefore in terms of pressure, we have

$$q = \frac{PA}{kD} = \frac{mg}{kD} \tag{12}$$

where P is the pressure, A is the surface area of the deformer mg is the weight and k is a constant.

General Procedure

1. We sandwich the fibre between two periods which will help induce microbending.
2. A weight pan is placed on top of the period
3. Weight on the pan is gradually increased and the cor- responding value for the intensity is noted.

Results

The results and the data recorded is tabulated in Table III and is plotted and fitted in Figure 15. After fitting the recorded data with equation 11, we obtained $C' = 8.489$ and $q = Ax = 5.588 \times 10^{-4}$ where $A = g/kD$.

E. Bend-induced loss in a single-mode fiber

The bending loss can be accounted for by the transition losses and the macrobend losses. Transition loss is due to the abrupt changes in curvature occurring, at the cross sectional plane of the fiber. The predominant effect of curvature on the fundamental mode is to shift the peak of the field distribution radially outwards (in the plane of the bend) by a distance r_d from the fiber axis.

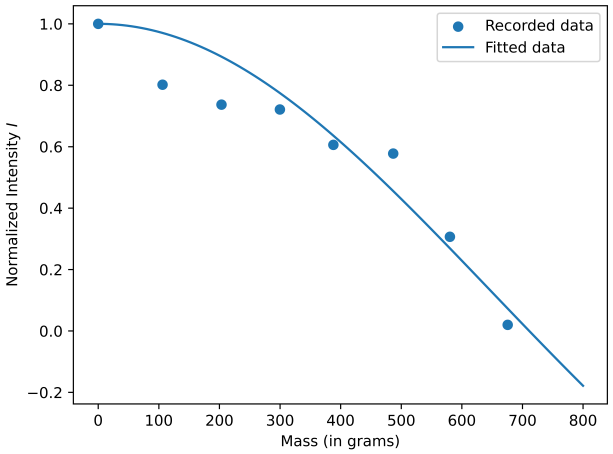

FIG. 15: Amount of light transmitted through a microbend-modulated fiber-optic sensor versus the applied weight.

The second mechanism of loss is the actual transmission loss suffered due to radiation from side of the bent fiber.The evanescent tail in the cladding decays almost exponentially with distance from the core-cladding interface. Since the evanescent tail moves along with the field in the core, part of the energy of a propagating mode travels in the fiber cladding.

The pure bend loss coefficient (in dB per unit length of the bent fiber) in a single moded step index fiber is given by:

$$\alpha \approx 4.34\left(\frac{\pi}{4aR_c}\right)^{1/2}\left(\frac{U}{VK_1(W)}\right)^2\frac{1}{W^{3/2}}\exp\left(-\frac{4}{3}\frac{R_c}{a}\frac{W^3\Delta}{V^2}\right) \tag{13}$$

Here $K_1(x)$ is is the modified Bessel function of second kind. The parameters U , W, V and Δ are defined through:

$$U = a\sqrt{k_0^2 n_1^2 - \beta^2}$$
$$W = a\sqrt{\beta^2 - k_0^2 n_2^2}$$
$$V^2 = U^2 + W^2$$
$$\Delta \simeq (n_1 - n_2)/n_2$$
$$k_0 = 2pi/\lambda$$

We wind the fibre around the spool and the absorption coefficient (α) is given by:

$$\alpha = -\frac{10}{L}\log\frac{P_2}{P_1} \tag{14}$$

where L is the length of the fiber (within the bend) i.e. $2\pi R\times$ (no. of turns), P_1 is the output power without the bend in the fiber and P_2 is the output power with the bend in the fiber.

We compare our curve to given theoretical equation:

$$\alpha = 1187.3\exp(-10.3941 * R)/R^{0.5} \tag{15}$$

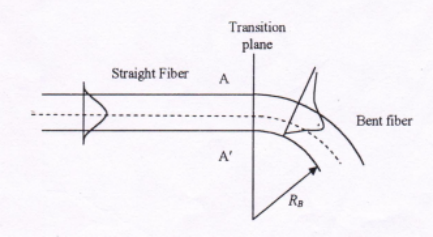

FIG. 16: A qualitative representation of the shift in the Gaussian-like fundamental mode away from the fiber axis at a bend.

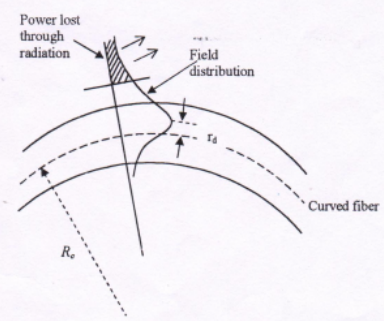

FIG. 17: Schematic representation of the bending loss in a section of fiber bent into an arc of radius R_c

General Procedure

1. After coupling the fibre to the 20X microscope, we measure the maximum output through the detector

2. Then the optical fibre is wound on the top of the first spool. First a single turn is done and output is recorded. Other objects such as brass rod, or pen were also used to induce bends.

3. Then the process is repeated on the larger radius sec- tion of the spool.

4. The data is fitted to the given theoretical curve.

Results

We recorded and tabulated the data in Table IV and plotted and fitted the data in Figure 19.

V. RESULTS, DISCUSSIONS AND CONCLUSIONS

1. The numerical aperture for single-mode fiber was calculated to be 0.172.

2. The numerical aperture for multi-mode fiber was calculated to be 0.2310.

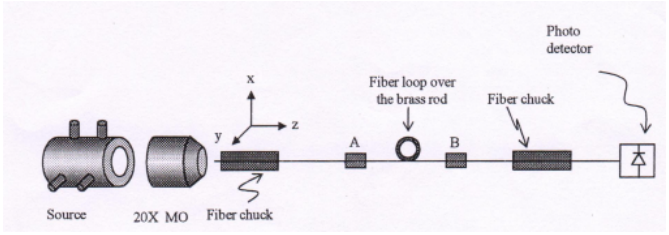

FIG. 18: Experimental setup to study the macro-bending loss in a single mode fiber

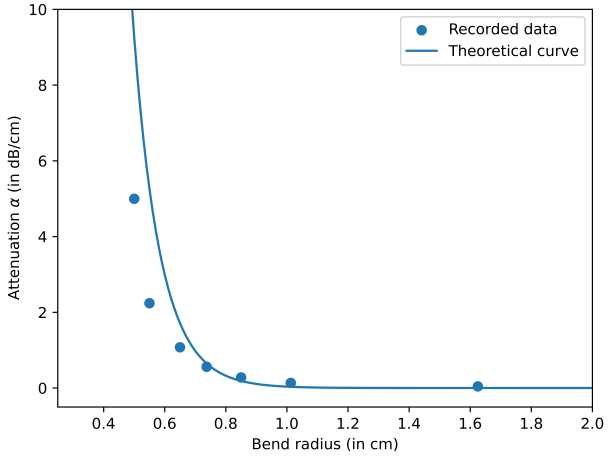

FIG. 19: Bend loss of a single mode step-index fiber as a function of bend radius.

3. The mode-field diameter of the single-mode fiber was calculated to be 1.4 µm.

4. We successfully studied and fitted the trend for microbending loss in a multi-mode fiber.

5. We successfully studied and fitted the trend for bend-induced loss in a single-mode fiber.

6. In a multimode fiber, different mode groups suffer different attenuation rates, which is referred to as differential mode attenuation (DMA). Therefore the NA measured by visual means is generally a bit inflated.

7. In addition, NA is critically dependent on the excitation conditions. To ensure that all the guided modes are excited in a multimode fiber, an "overfill launch" is applied at the input end i.e. one uses a microscope objective of NA higher than that of the fiber for launching light into the fiber. This results in the excitation of the cladding modes and the radiation modes, which quickly lose power as they propagate along the fiber.

8. he analyses discussed under the theory section are based on meridional rays. However, a greater power

TABLE IV: Recorded data for bend-induced loss in single-mode fiber

Diameter D (in cm)	Radius $r = D/2$ (in cm)	Bend length ($L = 2\pi r$) (in cm)	Voltage V (in volts)	Voltage loss ΔV V/V_{max}	Power loss ΔP ($\propto (\Delta V)^2$)	Attenuation α (in dB/cm)
1.000	0.5000	3.142	0.062	0.164	0.027	4.998
1.100	0.5500	3.456	0.155	0.410	0.168	2.241
1.300	0.6500	4.084	0.228	0.603	0.364	1.075
1.475	0.7375	4.634	0.280	0.741	0.549	0.563
1.700	0.8500	5.341	0.318	0.841	0.708	0.281
2.025	1.0125	6.362	0.342	0.905	0.819	0.137
3.250	1.6250	10.210	0.359	0.950	0.902	0.044

loss arises when skew rays are included in the analyses, since many of the skew rays that geometric optics predicts are trapped in the fiber are actually leaky rays. These leaky rays are only partially confined to the core of the circular optical fiber and attenuate as the light travels along the fiber. Thus, a detailed inclusion of skew rays will change the expression of the light acceptance ability (NA) of the fiber.

9. It is necessary that the far-field intensity pattern be detected at a sufficiently large distance from the center of the fiber output end such that good angular resolution is achieved in detection.

10. Fiber optics also provided a revolutionary technology base for configuring a variety of optical sensors, which offer several! advantages over existing traditional sensing techniques. These optical sensors are direct consequences of the physical effects we studied through micr-bending loss.

11. One of the most important parameters in determining the microbending sensitivity is the periodicity of the fiber deformation. To understand this, one has to consider the mode coupling effects in fibers.

VI. PRECAUTIONS

1. The fiber end faces must be of good quality.

2. Cladding-mode strippers must be used.

3. The output end of the fiber must be positioned in such a way that the axis of the rotation of rotation stage passes through it.

4. The two plates of the deformer must be accurately aligned.